Imaging and Radiation Research (2020) Volume 3 Issue 1
doi:10.24294/irr.v3i1.1722

REVIEW ARTICLE

Imaging diagnostics of gynecological emergencies

Matthias W. Wagner, Thierry A. G. M. Huisman, Rahel A. Kubik*

MPH, Institut für Radiologie, Kantonsspital Baden AG, Im Ergel 1, CH-5404 Baden, Switzerland. E-mail: rahel.kubik@ksb.ch

ABSTRACT

Acute abdomen is a frequent clinical picture in emergency diagnostics. Pathologic changes of the female genital organs play an important role. Gynecologic emergencies threaten fertility and are potentially life-threatening. Many differential diagnoses must be considered in the diagnostic process, depending on the age of the patient and any pregnancy. In particular, acute gastrointestinal symptoms often cannot be differentiated from gynecologic emergencies on clinical examination. Here, imaging makes a significant contribution to narrowing the differential diagnosis, making treatment decisions, and monitoring therapy. This review article will discuss the central role of imaging in the context of common gynecologic emergencies.

Keywords: Emergency; Gynaecology; Imaging; Ovary; Uterus

ARTICLE INFO

Received: 5 January 2020
Accepted: 23 February 2020
Available online: 2 March 2020

1. Introduction

Acute diseases of the female genital organs are a common cause of acute abdomen[1]. Because of the many possible differential diagnoses, clinical examination is often insufficient to differentiate gynecologic and gastrointestinal emergencies (e.g., appendicitis). An additional diagnostic challenge is the workup of emergencies during pregnancy. Common findings in a normally progressing pregnancy, such as nausea, vomiting, or nonspecific pain, influence the clinical presentation and complicate the clinical picture. In addition, the clinical examination of a pregnant patient is more difficult to assess, and laboratory parameters such as CRP and leukocytes are elevated in the setting of pregnancy. As a result, imaging is becoming increasingly important in emergency diagnostic workup, which is reflected not least in the steadily rising number of examinations. In the USA, the frequency of using diagnostic imaging during pregnancy has doubled within the last decade[2]. Depending on the suspected diagnosis, various imaging techniques are used:

(1) Ultrasound (US) is initially the imaging method of choice, regardless of whether pregnancy is present or not.

(2) CT has its importance in the workup of acute trauma.

(3) MRI is used in unclear and subacute cases or for diagnosis in pregnancy[3].

In general, imaging is readily available, which can objectify the clinical diagnosis of suspicion, and can also monitor emergencies during their course, if necessary. However, a detailed medical history (e.g., previous operations, previous pregnancies) and a detailed clinical ex-

amination are the first step in any clarification. Used in a targeted manner, radiological diagnostics can confirm and exclude suspected diagnoses or point to other underlying changes.

This review article is intended to

(1) provide an overview of the different presentations of gynecologic emergencies on ultrasound (US), CT, and MRI,

(2) recommend the imaging method of choice depending on the suspected clinical diagnosis,

(3) assist in the interpretation of imaging findings in a clinical context to ensure adequate patient care, and

(4) refer to the current guidelines on the use of contrast media during pregnancy and lactation.

2. Methods

2.1 Ultrasound

Indications. Ultrasound (US) is characterized by high sensitivity in many acute diseases. In addition, it is cost-efficient and quickly available, so that it is often used for the initial examination of the patient. The transabdominal ultrasound is usually performed by the radiologist. Depending on the patient's habitus, it is possible to obtain information about the uterus and the adnexa, but above all about pathological changes such as free fluid in the abdomen. Differential diagnoses such as urinary retention or appendicitis can be excluded. A more accurate assessment of the genital organs themselves is achieved with transvaginal sonography[4]. Significant additional information can be obtained with the aid of color Doppler. For example, color Doppler is of decisive importance in the question of organ perfusion.

Pregnancy. There are no known adverse effects of sonography on the mother or fetus. However, the US Food and Drug Administration (FDA) recommends a maximum sound wave intensity of 720 mW/cm^2 during pregnancy. This intensity may well be reached during a Doppler examination. Therefore, Doppler ultrasound should be used for as short a time as possible—just long enough for the diagnosis to be made[5].

Contrast media. Contrast media for sonography consist of gas-filled microbubbles surrounded by an elastic shell. This envelope consists of lipids, albumin, polymers or other excipients such as surfactants or polyethylene glycol. The contrast media are usually administered intravenously and are respirable. Primarily, they distribute in the vessels and thus exhibit high contrast demarcation from the extravascular space. They are extremely well tolerated, but are not currently used in children or pregnant women[6,7]. Ultrasound contrast agents are generally not used in gynecologic emergencies.

2.2 Computed tomography

Indications. Due to radiation exposure, CT should be avoided—especially in younger and pregnant patients. The likelihood of teratogenic effects from ionizing radiation increases with the dose applied. However, modern CT protocols ("low dose CT") do not reach the limits determined for teratogenic effects. A strict risk-benefit analysis for the mother and the fetus is required before any CT examination. Under no circumstances should CT be used as a search method for unclear findings. In an acute life-threatening situation, however, it is the method of first choice.

Contrast media in pregnancy. In animal studies, water-soluble iodine-containing contrast media had no teratogenic effect when administered intravenously. However, parenteral injection, especially after the 12th week of pregnancy, increases the risk of neonatal hypothyroidism. Therefore, the European Society of Urogenital Radiology (ESUR) guidelines recommend[5,8]:

(1) apply iodine-containing contrast medium only if absolutely necessary.

(2) screen for neonatal hypothyroidism in the first week after birth.

Regardless of the patient's pregnancy status or age and sex, one should ask before any imaging whether ionizing radiation is needed to answer the question, contrast material is critical, and imaging results will change therapy.

2.3 Magnetic resonance imaging

Indications. In the diagnosis of the female pelvis, MRI is superior to CT as an adjunct to ul-

trasound in several respects. Radiation exposure is absent, soft tissue contrast is higher, and a variety of contrasts can be obtained. To date, there is no evidence of increased risk to the fetus with MRI at 1.5T or lower magnetic field strength. However, due to limited data, this only applies to the second and third trimesters. As a precaution, MRI should therefore be avoided in the 1st trimester or—depending on the maternal indication—weighed particularly carefully. The safety of 3T devices has not yet been adequately confirmed, but there are no reports of adverse effects. Animal studies with stronger magnets (>3T) and prolonged exposure time did not reveal teratogenic effects[5]. Nevertheless, pregnant women should be informed in detail before any MRI or CT examination and this information should be documented in writing.

Contrast media in pregnancy. Although data are limited, it appears that the application of gadolinium-containing contrast media has no adverse effects on the fetus. Gadolinium crosses the placental barrier and is excreted into the amniotic fluid via the fetal kidneys. The FDA recommends the use of gadolinium-containing contrast agent only if the risk-benefit ratio is positive. The lowest possible dose of a stable, macrocyclic contrast agent should then be used (**Table 1**)[5,8]. However, a correct diagnosis is possible in most cases even without contrast medium, so we do not administer any contrast medium during pregnancy.

In gynecological emergencies, US and MRI are basically the methods of choice. If CT is used, e.g., for an acute abdomen, the radiation dose should be kept as low as possible (ALARA principle). MRI is reserved for subacute clinical pictures and is mainly used to clarify sonographically unclear findings. A positive risk-benefit ratio may justify the use of CT and MRI in rare cases, as well as the use of contrast media in pregnancy.

Table 1. Radiation dose and contrast media during pregnancy and lactation

Phase	Radiation dose and contrast medium
Pregnancy[8,9]	CT ■ ionizing radiation - teratogenic risk minimal at fetal dose <100 mGy - increased relative risk of neoplasia resulting in death ■ Contrast media containing iodine - in exceptional cases—only if absolutely indicated - checking the thyroid function of the newborn within the first week after birth MRI ■ relative contraindication in the 1st trimester gadolinium-containing contrast media ■ in exceptional cases—only if absolutely indicated ■ smallest possible dose of the most stable macrocyclic contrast agent ■ no further tests necessary for newborns ■ in case of impaired renal function: do not use contrast media containing gadolinium
Lactation[8,9]	■ CT: after iodine-containing contrast medium, breastfeeding can continue unchanged. ■ MRT: with stable macrocyclic gadolinium preparations, breastfeeding can continue unchanged

3. US/CT/MRI contrast media in the breastfeeding period

3.1 Ultrasound contrast agent

Breastfeeding can be continued normally after administration of the ultrasound contrast media, which is rarely mandatory in clinical practice.

3.2 Iodinated and gadolinium-containing contrast media

Iodinated and gadolinium-containing contrast media are excreted in breast milk at approximately 0.5% of the administered dose within the first 24 hours. As a result, less than 1 % of the amount of contrast medium absorbed by the child with the breast milk is absorbed in the child's intestine. The exposure of the newborn is therefore negligible. With regard to iodide exposure, there are no reports of increased sensitization, allergy rates or late reactions in newborns.

If gadolinium is used during breastfeeding, the more stable macrocyclic complexes are recommended. According to the ESUR guidelines, breastfeeding can be continued unchanged[5].

For the linear, more unstable gadolinium preparations, the ESUR guidelines recommend

not breastfeeding for at least 24 hours after contrast administration. However, the study by Kubik *et al.* showed that breast milk contains gadolinium for more than 48 hours after parenteral administration of a linear gadolinium preparation[10]. Accordingly, a break in breastfeeding of only 24 hours is not sufficient to avoid systemic exposure of the newborn to the linear contrast agent[5,8]. It follows that macrocyclic gadolinium should be preferred during pregnancy.

4. Gynecological clinical pictures

4.1 Hematometrocolpos

In hematometrocolpos (HMK), the vagina and uterus are distended and filled with blood. The incidence of HMK in teenagers is approximately 1:1,000~2,000, with about two-thirds of all cases resulting from hymenal atresia. Other possible causes include cloacal malformations and anomalies of the Müllerian ducts, e.g., a transverse septum in a didelphys uterus[11]. The diagnosis of a HMK is mostly made during prenatal diagnosis, immediately after birth or with the onset of puberty. Typical symptoms at the onset of puberty are abdominal pain associated with primary amenorrhea[12,13].

Ultrasound. On ultrasound, the uterus can be delineated with mixed echogenic, majority echo-rich intraluminal fluid. In marked findings, hydro/hematosalpinx may also be seen[13–15]. On US examination, one should also look for associated renal malformation or hydronephrosis. Transabdominal ultrasound is usually used, as transvaginal ultrasound is not performed in virgos. A possible but rarely used alternative is transrectal ultrasound.

Sonography shows a dilated uterus with a majority of echo-rich fluid in HMK. At the same time, associated renal malformation and hydronephrosis should be excluded.

CT. CT is often used initially in the search for the causes of acute abdominal pain. However, US and MRI are preferred in the suspected diagnosis of HMK. On CT, an HMK is a more-or-less hyperdense, noncontrast fluid-filled mass. The extension can be up to 25 cm[16].

MRI. MRI is the most informative method due to the better soft tissue contrast. It is mainly indicated when a complex malformation is suspected or a surgical intervention is planned[13,14,17]. Depending on the age of the hemorrhage, the signal intensity of the blood varies. In the subacute stage, blood on T1w and T2w images is usually hyperintense, whereas in the chronic stage it is hypointense (**Figures 1–3**).

MRI is indicated in an HMK when complex malformations are suspected or to prepare for surgical intervention.

4.2 Adnextorsion

Torsion of the adnexa is a rare emergency. It affects 2.7~7.4% of all women with acute abdominal pain[18,19]. Approximately 71% of all adnexal torsions occur between the ages of 20 and 39 years[20]. Torsion initially prevents venous and lymphatic return and later impairs arterial supply to the adnexa. Possible consequences are thrombosis, ischemia, and hemorrhagic infarction of the adnexa[21,22]. Early diagnosis is of paramount importance for preserving fertility. Adnexal torsions are more common on the right side (55~71%) and involve both the ovary and uterine tube (72%)[23,24]. In 50~90 % of all cases, the torsion is due to an ovarian mass:

(1) teratomas (17.2%)
(2) paratubal cysts or hydrosalpinx (16.7%)
(3) follicular cysts (15.9 %)
(4) cystadenomas (13.8%)
(5) also (more rarely): corpus luteum cysts, primary or secondary tumors, adhesions, or extrauterine pregnancy (EUG).

In children, it is usually a hypermobile adnexa without underlying disease. The risk of torsion increases significantly in ovarian cysts from a pole distance of 5 cm[19].

Ultrasound. Primary sonographic diagnosis can be made in 46~74%[25]. Signs of adnexal torsion are enlarged ovaries (>4 cm) with marginal follicles and free fluid in the Douglas space[22,24,26]. The marginal bead-like arrangement of follicles is called “string-of-pearls” sign and occurs in 12~74% of all cases. Duplex sonography frequently (13~88%) demonstrates a “whirlpool” sign caused by torqued

arterial and venous vessels. However, the ovarian Doppler signal is prone to error: it was normal in 45~61% of all cases with surgically confirmed adnexal torsion (**Figure 4**)[21,22,26–28].

Figure 1. 12-year-old female patient with cloacal malformation. The arrow shows isointense fluid accumulation in the T2w sequence in dilated vagina and uterus. The arrowhead indicates associated hydronephrosis. The asterisk marks an incisional renal cyst on the left. **a**, **b**: fat-saturated T2w sequence in coronary slice guidance; **c**: fat-saturated T2w sequence in axial slice guidance.

CT. In the case of torsion, CT is diagnostically inferior to ultrasound[24]. Torsion is indicated by enlarged, wall-thickened adnexa, ascites, deviation of the uterus ipsilaterally, and adjacent adipose tissue fibrosis[24,29,30].

MRI. MRI is indicated in patients with subacute symptoms and unclear US findings[22,31]. Its soft tissue contrast is higher compared with CT, allowing better visualization of free fluid in the Douglas space, enlarged ovaries (>4~5 cm) with marginal follicles, periovarian edema and hematoma, and hemorrhagic infarction of torqued adnexa[25,28]. The findings with the highest sensitivity on MRI are uterine tubal wall thickening (91%) and a “whirlpool” sign (68% of all cases)[18]. Regarding the additional benefit of diffusion-weighted imaging in adnexal torsions, larger studies are currently lacking. In a study of 12 patients, hemorrhagic infarction of torqued adnexal masses was associated with significantly increased diffusion restriction of the wall of the masses[32].

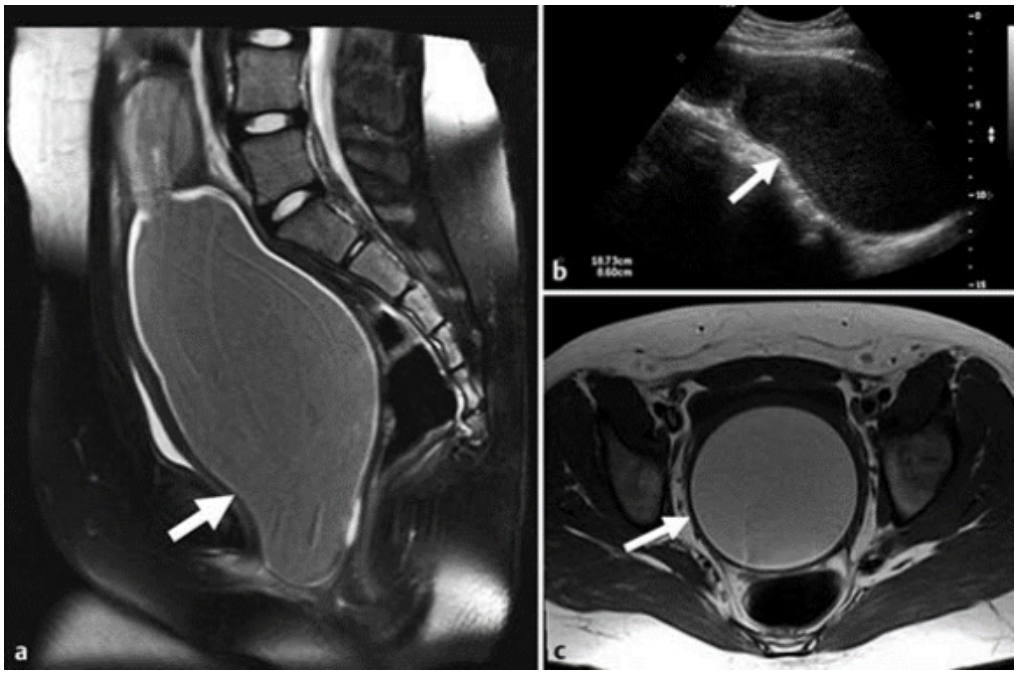

Figure 2. 11-year-old female patient with hematocolpos in hymenal atresia. The arrow indicates hypoechogenic or, in the T1w sequence, hyperintense, and in the T2w sequence, isointense fluid accumulation in the dilated vagina. **a**: sagittal T2w sequence; **b**: transabdominal ultrasound; c: axial, T1w sequence.

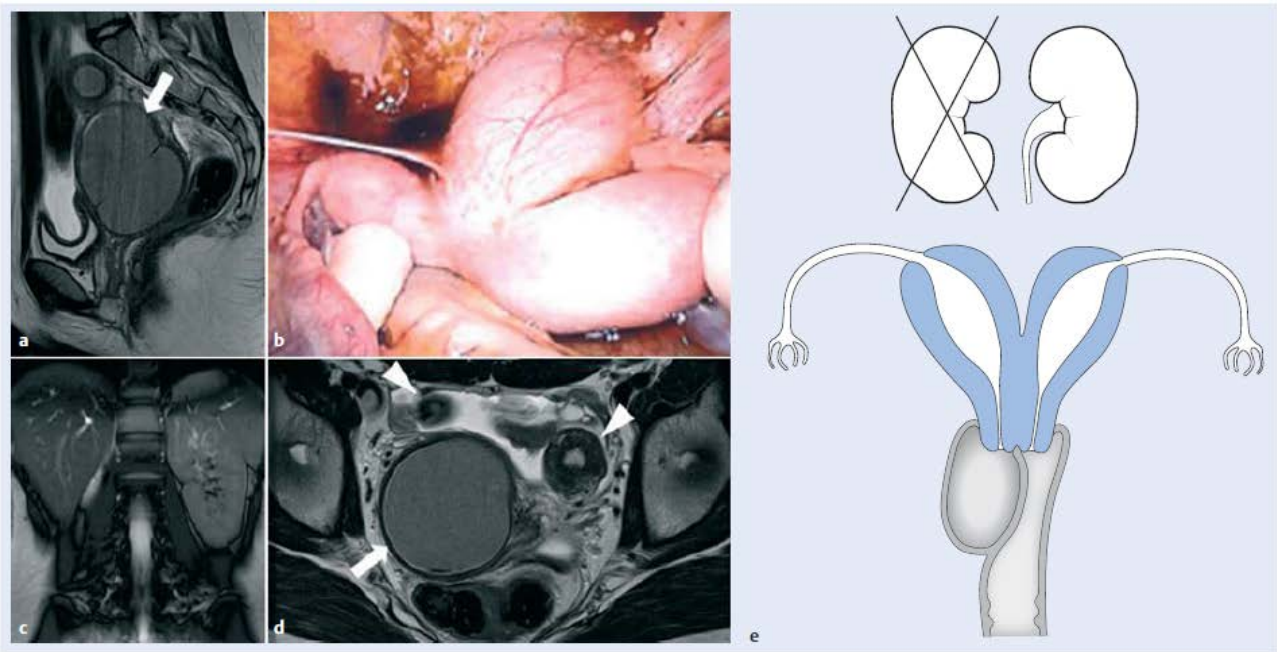

Figure 3. 13-year-old female patient with uterus didelphys, renal agenesis on the right and transverse vaginal septum with hematometrocolpos. The arrow marks the hematometrocolpos, the arrowheads in the uterus didelphys. **a**: sagittal, T2w sequence; **b**: intraoperative situs with dilated vagina; c: coronary TrueFISP sequence, renal agenesis on the right; **d**: axial TrueFISP sequence; **e**: schematic of malformations: uterus didelphys, right renal agenesis, and transverse vaginal septum (from Emans *et al.*[33]).

4.3 Pelvic inflammatory disease

Pelvic inflammatory disease (PID) is an acute clinical syndrome caused by ascending infection of microorganisms (e.g., chlamydia, neisseria). PID begins in the vagina or cervix and ascends through the endometrium to the uterine tuba and ovary. Approximately one-third of all patients hospitalized for PID develop adnexitis (combined salpingitis and oophoritis).

4.3.1 Tuboovarian abscess

If PID is treated too late or inadequately, a tuboovarian abscess (TOA) may develop[34,35]. On

imaging, it is sometimes difficult to differentiate this abscess from ovarian neoplasia. Clinical features such as fever, leukocytosis, or motion-related cervical pain may be informative.

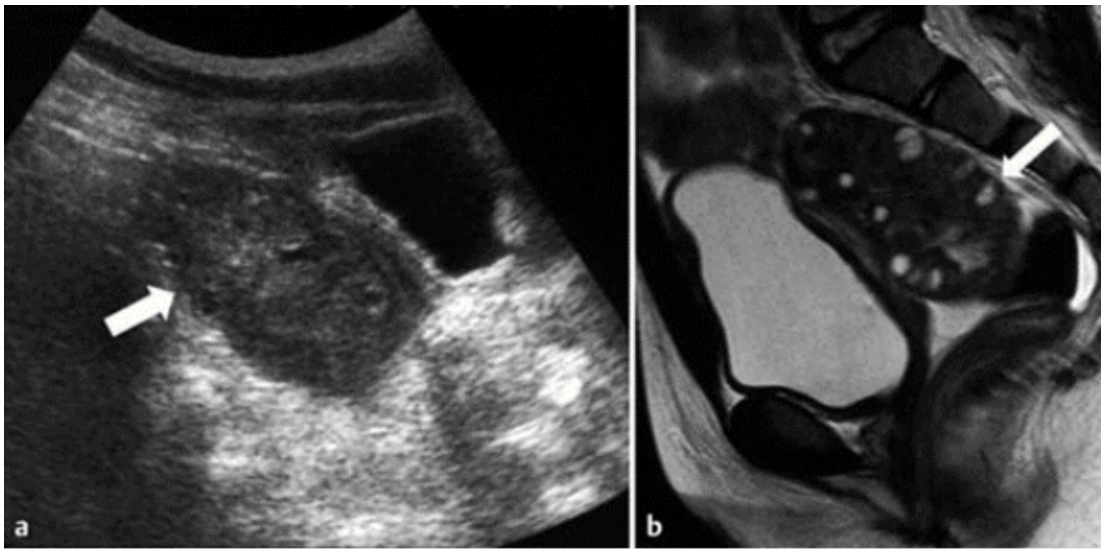

Figure 4. 6-year-old female patient with adnexal torsion. **a**: transabdominal ultrasound: the arrow points to the predominantly hypoechogenic mass craniodorsal to the urinary bladder with dorsal sound enhancement; **b**: sagittal T2w sequence: the arrow shows the enlarged ovary with marginal follicles. Additionally, some fluid is found in the excavatio rectouterina.

Ultrasound. US is highly sensitive (83~100%) and specific (83~98.6%) for the detection of TOA in retrospective studies[36]. Common findings include solid and/or cystic space lesions and free fluid in the adnexal region and Douglas space. In addition, the uterus loses its sharp outer contour and the endometrial echo may be absent[37].

On US, a TOA reveals solid and/or cystic masses as well as free fluid in the adnexal region and Douglas space.

CT. On CT, TOA appears as wall-thickened fluid collections with marginal contrast uptake[34,37–39]. The mesosalpinx is thickened and deviates ventrally (91~100%)[34,37]. The fat lamella between the abscess and adjacent organs (rectum, sigmoid colon, ureter) is obliterated (58~91%)[34,35,38,39]. Thickened uterosacral ligaments (45~66%), a pyosalpinx (50%), and extraluminal free air (12.5%) are also indicative of TOA[34,37–39].

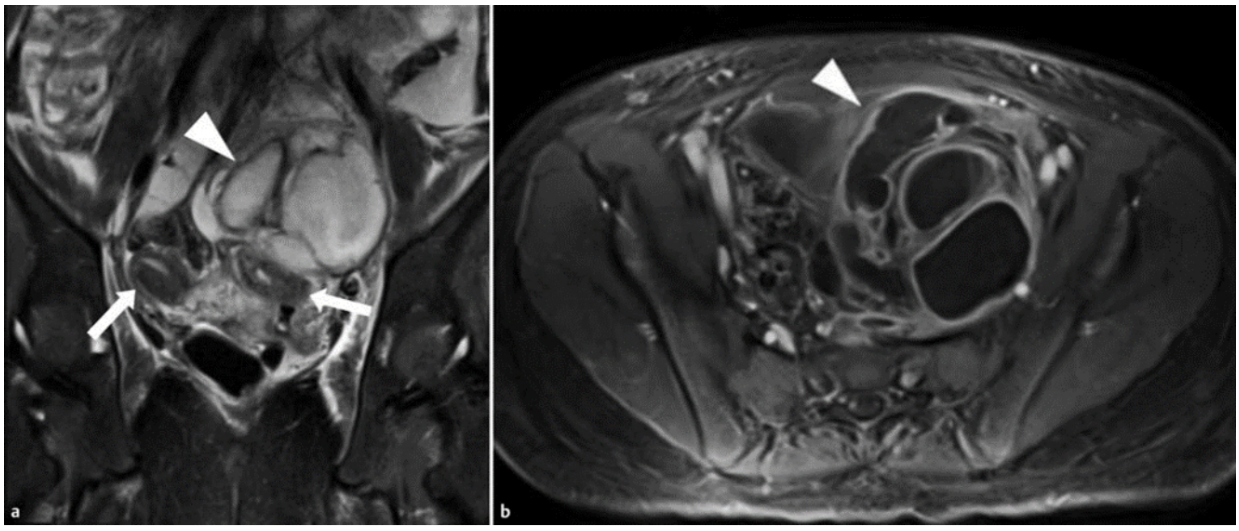

Figure 5. 15-year-old female patient with uterus didelphys and tuboovarian abscess. The arrowhead points to the marginally contrast-enhanced, polylobulated mass corresponding to the tuboovarian abscess. **a**: coronary, fat-saturated T2w sequence, the arrows mark the uterus didelphys; **b**: axial, contrast-enhanced, fat-saturated T1w sequence.

Helpful for the differential diagnosis of TOA and ovarian cancer is the clinical picture of the patient (e.g., signs of inflammation) and the MRI.

MRI. MRI has the highest sensitivity and specificity for abdominal abscesses (100% and 94%, respectively)[40]. TOA is usually hypointense on T1w and mixed hyperintense on T2w images[41,42]. The abscess capsule is best detected on the contrast-enhanced, fat-saturated T1w sequence[40]. The signal intensity of the abscess contents depends on their protein concentration. Some hyperintense hemorrhagic granulation tissue is often found inside the T1w sequence[42]. The usually blurred demarcated spread of the inflammatory reaction is hyperintense on T2w images and isointense on the fat-saturated, contrast-enhanced T1w images[41]. The data on the differential diagnosis of ovarian cancer using diffusion-weighted imaging is not uniform to date (**Figure 5**)[43,44].

MRI is the best method for diagnosing intraperitoneal abscesses. The abscess is hypointense on T1w and hyperintense on T2w images. For perifocal inflammatory response, T2w sequence and contrast-enhanced fat-saturated T1w sequence are helpful.

4.3.2 Postpartum ovarian vein thrombosis

Postpartum septic ovarian vein thrombosis (SPOVT) is another rare complication of PGD. The prevalence is 0.15~0.18% within the postpartum population[45]. The incidence is 1:9,000 after vaginal delivery and 1: 800 after caesarean section[46]. Basically, both ovarian veins can thrombose, but the right side is more frequently affected[45]. SPOVT is often a diagnosis of exclusion in postpartum persistent fever. Therapeutically, broad-spectrum antibiotics are applied parenterally; systemically, low-molecular-weight heparin is used for anticoagulation[47,48].

Ultrasound. US can be used to delineate the enlarged ovary with an adjacent dilated tubular structure. Postpartum, dilated ovarian veins are common, so Doppler should be used to check venous flow. If the findings are unclear or the flow signal is absent, CT or MRI are indicated[49]. The ovarian veins are difficult to visualize continuously in their course, but the proximal insertion to the inferior vena cava can often be seen.

CT. In contrast-enhanced CT, the diagnosis of SPOVT is easier to make. An intraluminal hypodense structure in a dilated vessel corresponds to fresh thrombus. In addition, a contrast-enhancing vessel wall is found from the ovary to the inferior vena cava on the right side or to the renal vein on the left side. Adjacent fat tissue impaction is possible (**Figure 6**).

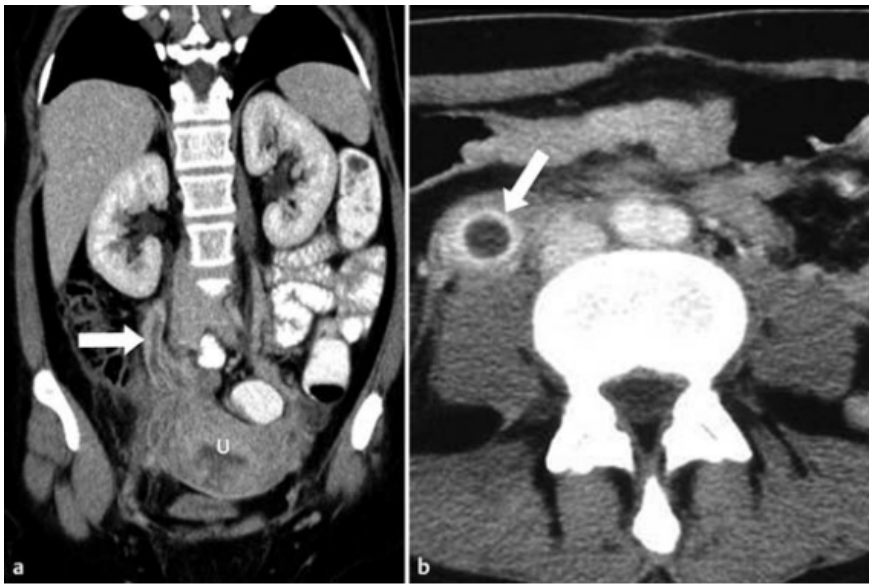

Figure 6. Septic postpartum ovarian vein thrombosis (SPOVT). The arrow marks the dilated, marginally contrast-enhancing ovarian vein with intraluminal hypodense filling defect (= thrombus) and adjacent imbibed adipose tissue. **a**: coronal reformat of a contrast-enhanced CT, U = uterus; **b**: axial plane of a contrast-enhanced CT.

MRI. On MRI, the thrombus is seen as a hypointense filling defect on contrast-enhanced, T1w images and hyperintense on T2w images. In the diffusion-weighted sequence, there is restriction of the thrombus[50]. The advantage of diffusion-weighted as well as time-of-flight (TOF) angiography is the saving of contrast agent compared with conventional MRI sequences and CT[50].

4.4 Extrauterine pregnancy

Extrauterine pregnancy (EUG) is the most common emergency in early pregnancy. The diagnosis is usually made by human chorionic gonadotropin (hCG) measurement and transvaginal ultrasound (TVUS). With a decreasing mortality rate, the incidence of EUG has been increasing in recent decades[51]. Risk factors of EUG include "pelvic inflammatory disease", endometriosis, previous gynecologic surgery, infertility therapy, late primiparity, and assisted reproductive therapies (artificial insemination, in vitro fertilization).

Nearly all EUGs occur in the uterine tuba: 55% in the ampulla, 25% in the isthmus, and 17% in the fimbriae[52]. Other very rare sites of manifestation (approximately 3% of all cases) include the cervix uteri, scars after caesarean section, congenital rudiments, and the abdominal cavity[53]. In the context of assisted reproductive therapies, the rarer sites of manifestation of EUG are increasing slightly (**Figure 7**)[54,55].

Ultrasound. Due to its very high sensitivity and specificity (69~99% and 84~99.9%, respectively), its high availability, and its cost-effectiveness, transvaginal ultrasound is the method of choice for EUG[56–60]. In up to 57.9% of cases, EUG can be delineated as a small solid, inhomogeneous mass ("blob" sign) in close proximity to the ovary[57]. A "tubal-ring" sign (EUG as a hyperechogenic ring) was reported in 20.4% and a gestational sac with a fetal pole in 13.2%[57]. However, hematometra, hematoperitoneum, or patient agitation with severe pain significantly limit the usefulness of US.

Transvaginal ultrasound is the diagnostic method of choice for EUG. Ultrasound signs of EUG are the "blob-sign" and the "tubal ring-sign".

CT. Although CT is often requested for the workup of an acute abdomen, it should be avoided in pregnant women. CT criteria for EUG essentially correlate with US findings.

MRI. MRI is used for clarification in unclear cases. Hematometra is a diagnostic finding for EUG and presents iso-/hyperintense on T1w images, with mixed signal on T2w images, and with susceptibility artifacts on T2*w images. The EUG itself presents as a solid-appearing mass isointense in the T1w sequence and mixed iso- to hypointense in the T2w sequence (**Figure 8**)[61].

The hematometra typical of EUG is iso-/hyperintense on T1w recordings and shows mixed signal behavior on T2w and susceptibility artifacts on T2*w recordings.

4.5 Leiomyomas

Leiomyomas are benign tumors consisting mainly of smooth muscle and a variable proportion of fibrous connective tissue. Leiomyomas are the most common gynecological neoplasms and occur in 20~30% of all women of childbearing age. Depending on the localization, a distinction is made between submucosal, intramural, or subserosal leiomyomas[62]. Submucosal and subserosal leiomyomas tend to have pedunculated growth with increased risk of torsion, infarction, and necrosis[63]. Leiomyomas are considered parasitic when neovascularization occurs over extrauterine structures after torsion of the vascular pedicle. Due to hormonally accelerated growth, leiomyomas become symptomatic more frequently during pregnancy and the incidence of torsion is increased[5,64]. Leiomyomas can degenerate in several ways. The most common variant, accounting for approximately 60% of all cases, is hyaline degeneration[65]. However, cystic, myxoid, and red degeneration are also possible. The latter presents clinically during pregnancy with an acute abdomen and is characterized by hemorrhagic infarction of the leiomyoma. Leiomyomas are the most common gynecologic neoplasms. The incidence of torsion of leiomyoma is increased during pregnancy. Red degeneration is a differential diagnosis for acute abdomen during pregnancy.

Ultrasound. On US, a solid mass with low echogenicity can be delineated. Calcifications appear as hyperechogenic foci with dorsal acoustic extinction[66]. Absence of flow signal on Doppler ultrasonography indicates stylet rotation[67].

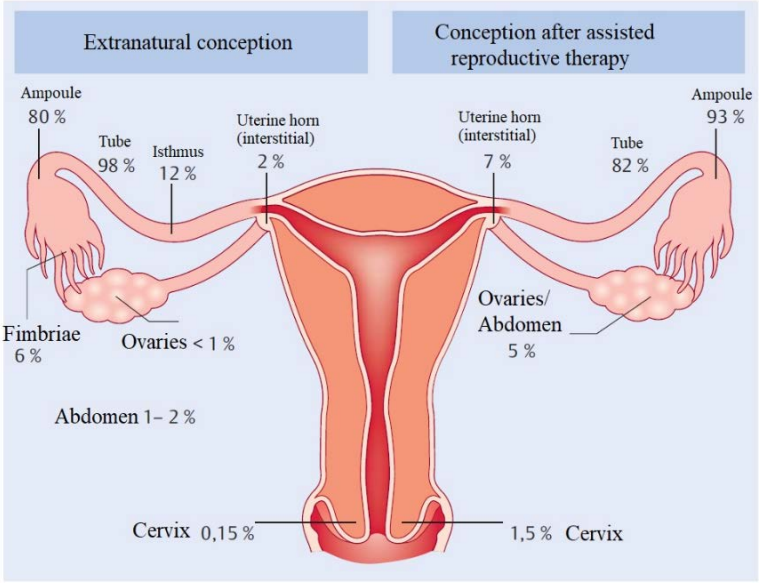

Figure 7. Distribution of extrauterine pregnancy with or without assisted reproductive therapy (from Hueppchen and Ling[68]).

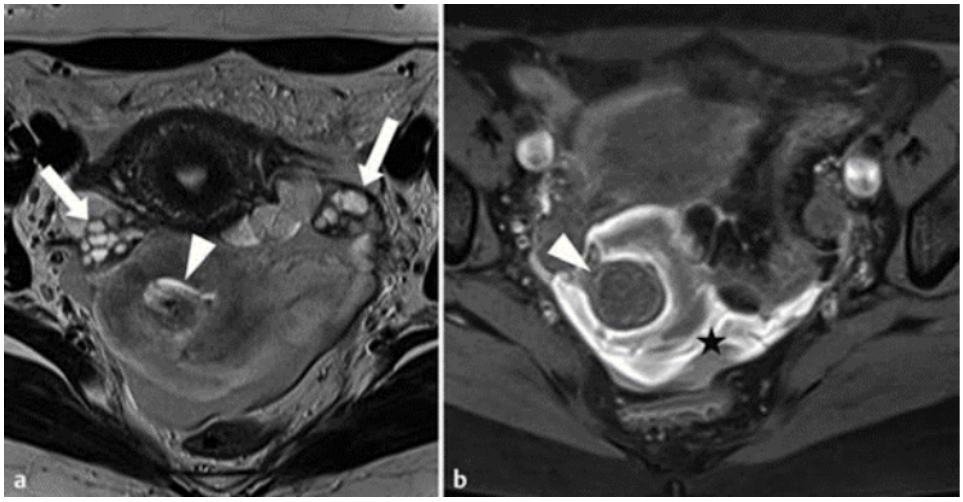

Figure 8. Ruptured EUG. The arrowhead points to a solid, in the T2w sequence, mixed iso/hypointense, in the T1w sequence isointense mass, corresponding to the EUG. A perifocal hematoma is marked by the asterisk. a: axial T2w sequence, the arrows mark the ovaries on the right and left, respectively; b: axial fat-saturated T1w sequence.

CT. On CT, degenerated and already necrotic leiomyomas appear centrally hypodense. On the edge, they take up contrast medium as a correlate for torqued veins or dilated, lymphatic vessels. Infarction of a leiomyoma can be seen as a loss of perfusion. Subsequent hemorrhagic infarction appears hyperdense on native CT[67]. Edema around the torqued and infarcted leiomyoma is typical[69].

MRI. MRI has a key function when the leiomyoma can only be assessed to a limited extent on US. The key advantage of MRI is the easier anatomical assignment of the leiomyoma to the uterus compared to other methods. A “bridging vascular” sign can be detected in the pedunculated junction, which has a sensitivity of 76.9%. This refers to the visualization of supplying, torqued vessels that form a “vascular bridge” between the uterus and the fibroid. This bridge can be seen on T2w and on contrast-enhanced T1w images. Regardless of stalk rotation, a subserosal leiomyoma can be distinguished from tumors of other origin that are adjacent to the uterus. Leiomyoma has a vascular bridge,

whereas the other tumors do not[31,70]. If stalk rotation is present, venous outflow is obstructed first. The obstructed veins can be delineated as a perifocal halo with hypointense signal on T2w and with hyperintense signal on T1w images[65,71]. Leiomyomas in hyaline degeneration are often hypobis isointense on T1w sequence and hypointense to myometrium on T2w sequence[65]. Hemorrhagic infarction in red degeneration is hyperintense on T1w and T2w images (subacute), for example, depending on the timing of hemorrhage (**Figure 9**)[65,71]. As known from intracranial hemorrhages, the MR image of extracranial hemorrhages also changes over time. However, the morphology of extracranial hemorrhages follows less schematic sequences and is also more heterogeneous[72].

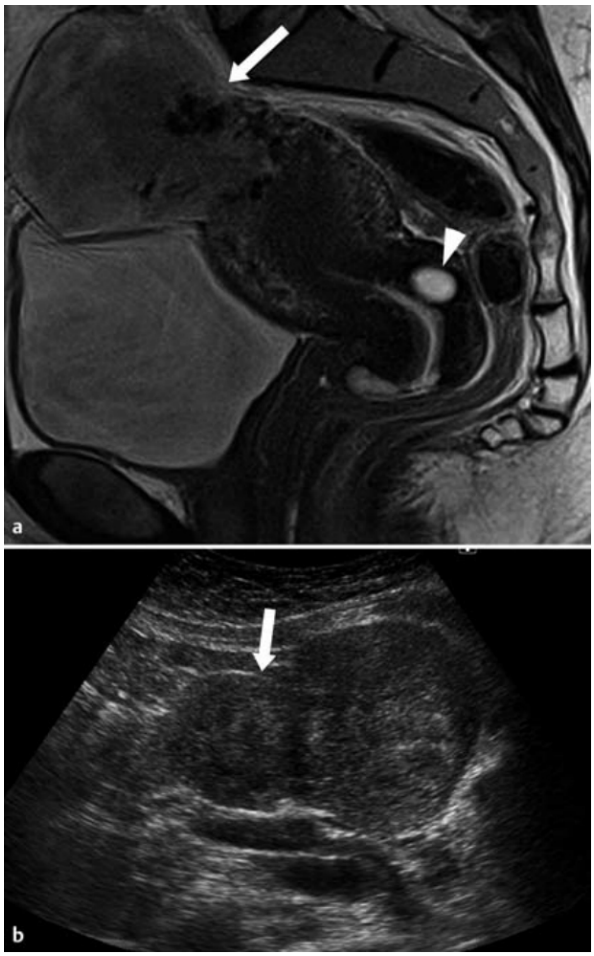

Figure 9. Torsion of a subserous leiomyoma. The arrow points to the isointense or mixed hyper- and hypoechogenic mass cranial to the uterus in the T2w sequence, corresponding to the torqued leiomyoma. The arrowhead points to an ovule Nabothi. **a**: sagittal, T2w sequence; **b**: transabdominal ultrasound.

On MRI, the visualization of infarction depends on the timing of hemorrhage. For example, in the subacute stage, it is hyperintense on T1w and T2w images. However, the overall signal behavior of extracranial hemorrhages is more heterogeneous than intracranial hemorrhages.

4.6 Uterine rupture

Uterine rupture is defined as a tear of the myometrium and serosa. In contrast, in uterine dehiscence, the serosa is still intact. Most often, intrapartum rupture is based on preexisting scarring of the myometrium, for example, after caesarean section. Rupture without preexisting scar is, for example, the result of trauma or congenital weakness of the myometrium (e.g., in Ehlers-Danlos syndrome type IV)[73,74]. Other causes include a protracted birth process or strong uterotonic drugs[75]. Symptoms of uterine rupture are nonspecific: there may be sudden pain between contractions, excessive vaginal bleeding with signs of shock, loss of uterine tone, and signs of fetal stress. In contrast,

uterine dehiscence is mostly asymptomatic, with occasional symptoms including dysmenorrhea, dyspareunia, chronic abdominal pain, and intermenstrual "spotting"[76].

A distinction is made between uterine rupture and dehiscence: in dehiscence, the serosa is still intact, whereas in rupture there is a connection between the uterine cavity and the peritoneal cavity. Dehiscence can be treated conservatively, whereas rupture usually requires surgery.

Ultrasound. US is prognostically useful to assess the risk of rupture in a future vaginal delivery after caesarean section. If the diameter of the uterus is less than 3.5 mm or that of the myometrium is less than 2 mm, this risk is significantly increased[5]. US findings of intrapartum uterine rupture include intraamniotic and/or extrauterine hematoma and extrauterine fetal body parts. Postpartum, the site of disruption cannot be identified by US, and findings tend to be nonspecific[5,76].

CT. On CT, there is an overlap with the expected normal postpartum findings. In *uterine dehiscence*, only nonspecific findings such as free fluid/air, pleural effusion, or bowel atony are found. Myometrial discontinuity is a normal finding immediately postpartum. Warning signs of uterine dehiscence include a "flap" hematoma greater than 5 cm and "streets" of free fluid/air with progression to intraperitoneal[76,77]. A "flap" hematoma refers to the hematoma formed at the peritoneal incision site between the bladder and myometrium during caesarean section. In the event of a rupture, the cavity uteri communicates with the peritoneal cavity, allowing air to accumulate intraperitoneally. Other more nonspecific warning signs of rupture include large volumes of hematoperitoneum or an infected "flap" hematoma. The "flap" hematoma is characterized by marginal contrast uptake, free air in the hematoma, and internal septation[77].

Free intra-abdominal air prepartum indicates uterine rupture.

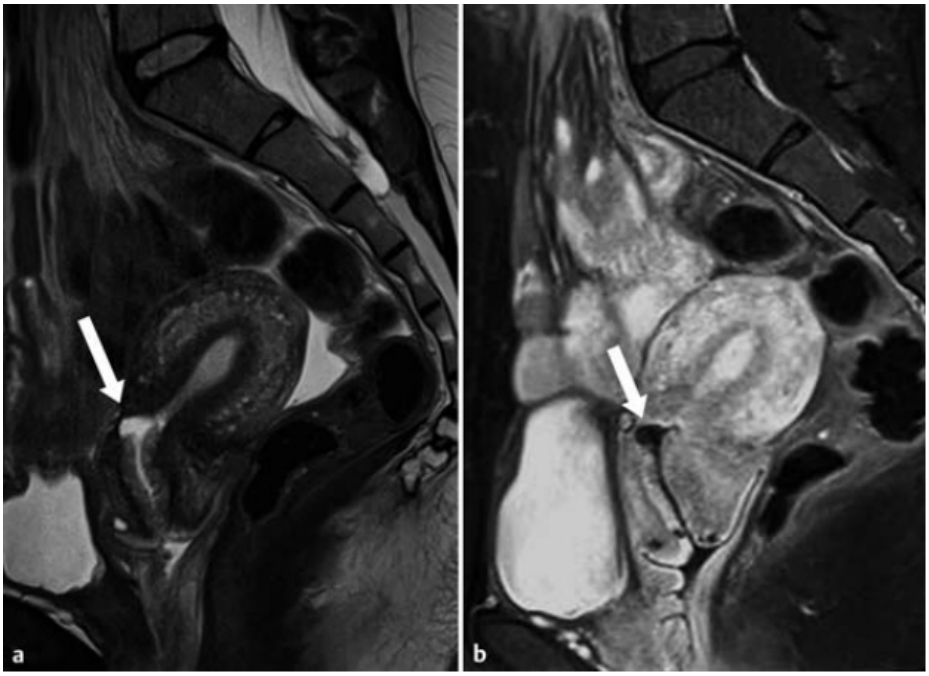

Figure 10. Uterine dehiscence. The arrow points to the hematoma in the presence of a focal tear of the myometrium and still intact serosa. **a**: sagittal, T2w sequence; **b**: sagittal, contrast-enhanced, fat-saturated T1w sequence.

MRI. MRI is the method with the highest informative method. It can differentiate between antepartum uterine rupture, uterine dehiscence, and uterine sacculations with functional weakness of the myometrium. Amniotic fluid and periuterine hemorrhages present iso/hypointense on T1w and hyperintense on T2w images[5,76]. The serosa is still delineable at *dehiscence* and prevents a "flap" hematoma from spreading. In contrast, in *rupture*, the serosa no longer appears continuous in the fat-saturated, T2w sequence[77]. The distinction between dehiscence and rupture is clinically rele-

vant because dehiscence can be treated conservatively, whereas rupture usually requires surgery. However, CT and MRI findings correlate poorly with operative findings in differentiating dehiscence from rupture (**Figure 10**)[77].

MRI allows delineation of the serosa in the fat-saturated T2w sequence and is therefore the more sensitive method for differentiating between dehiscence and rupture.

5. Core statements

(1) When CT is used on children, pregnant women or women of childbearing age, special attention should be paid to the radiation dose. The ALARA principle applies, i.e., the dose should be "as low as reasonably achievable".

(2) MRI is used to clarify subacute clinical pictures and unclear sonographic findings. If the indication is clear and the risk-benefit ratio is positive, MRI can also be performed in pregnant women.

(3) Hematometrocolpos (distended, blood-filled uterus and vagina) is caused by hymenal atresia in two thirds of all cases. After initial workup by ultrasound, associated renal malformation and hydronephrosis should be excluded.

(4) EUG is the most common emergency in early pregnancy and usually manifests in the uterine tube. Risk factors include pelvic inflammatory disease, endometriosis, and prior surgery. Ultrasound signs are a "blob-sign" and a "tubal ring-sign". MRI is used only to clarify unclear cases.

(5) Leiomyomas are the most common gynecologic neoplasms. Red degeneration of leiomyoma is an important differential diagnosis of acute abdomen during pregnancy. Torsion of a leiomyoma may also be a cause of acute abdomen.

Acknowledgement

We thank Dr. J. Fröhlich, Medical Director of Guerbet AG and ETH lecturer, Switzerland, for critically reviewing the information on contrast media and Prof. Dr. M. Hohl, Kantonsspital Baden, Switzerland, for providing **Figure 3b**.

Conflict of interest

The authors declare that they have no conflict of interest.

References

1. Roche O, Chavan N, Aquilina J, et al. Radiological appearances of gynaecological emergencies. Insights Into Imaging 2012; 3(3): 265–275.
2. Tirada N, Dreizin D, Khati NJ, *et al.* Imaging pregnant and lactating patients. Radiographics 2015; 35(6): 1751–1765.
3. Oto A, Ernst RD, Ghulmiyyah LM, *et al.* MR imaging in the triage of pregnant patients with acute abdominal and pelvic pain. Abdominal Imaging 2009; 34(2): 243–250.
4. Atri M, Leduc C, Gillett P, *et al.* Role of endovaginal sonography in the diagnosis and management of ectopic pregnancy. Radiographics 1996; 16(4): 755–774.
5. Masselli G, Derchi L, McHugo J, *et al.* Acute abdominal and pelvic pain in pregnancy: ESUR recommendations. European Radiology 2013; 23(12): 3485–3500.
6. Molins IG, Font JM, Alvaro JC, *et al.* Contrast-enhanced ultrasound in diagnosis and characterization of focal hepatic lesions. World Journal of Radiology 2010; 2(12): 455–462.
7. Nolsoe CP, Lorentzen T. International guidelines for contrastenhanced ultrasonography: Ultrasound imaging in the new millennium. Ultrasonography 2016; 35(2): 89–103.
8. Frohlich JM, Kubik-Huch RA. Radiographic, MR or ultrasound contrast media in pregnant or breast-feeding women: What are the key issues? RoFo 2013; 185(1): 13–25.
9. 9.0 Contrast Media Guidelines [Internet]. European Society of Urogenital Radiology; 2016. Available from: http://www.esur.org/esur-guidelines.
10. Kubik-Huch RA, Gottstein-Aalame NM, Frenzel T, *et al.* Gadopentetate dimeglumine excretion into human breast milk during lactation. Radiology 2000; 216(2): 555–558.
11. Posner JC, Spandorfer PR. Early detection of imperforate hymen prevents morbidity from delays in diagnosis. Pediatrics 2005; 115(4): 1008–1012.
12. Basaran M, Usal D, Aydemir C. Hymen sparing surgery for imperforate hymen: Case reports and review of literature. Journal of Pediatric and Adolescent Gynecology 2009; 22(4): e61–e64.
13. Fischer JW, Kwan CW. Emergency point-of-care ultrasound diagnosis of hematocolpometra and imperforate hymen in the pediatric emergency department. Pediatric Emergency Care 2014; 30(2): 128–130.
14. Dane C, Dane B, Erginbas M, *et al.* Imperforate hymen-a rare cause of abdominal pain: Two cases and review of the literature. Journal of Pediatric Adolescent Gynecology 2007; 20(4): 245–247.
15. Drakonaki EE, Tritou I, Pitsoulis G, *et al.* Hematocolpometra due to an imperforate hymen presenting with back pain: Sonographic diagnosis. Journal of

Ultrasound in Medicine 2010; 29(2): 321–322.
16. Poll LW, Flake P. Images in clinical medicine. Imperforate hymen with hematocolpometra. New England Journal of Medicine 2011; 365: 157.
17. Krafft C, Hartin Jr CW, Ozgediz DE. Magnetic resonance as an aid in the diagnosis of a transverse vaginal septum. Journal of Pediatric Surgery 2012; 47(2): 422–425.
18. Beranger-Gibert S, Sakly H, Ballester M, *et al.* Diagnostic value of MR imaging in the diagnosis of adnexal torsion. Radiology 2016; 279(2): 461–470
19. Damigos E, Johns J, Ross J. An update on the diagnosis and management of ovarian torsion. The Obstetrician & Gynaecologist 2012; 14(4): 229–236.
20. Hibbard LT. Adnexal torsion. American Journal of Obstetrics and Gynecology 1985; 152(4): 456–461.
21. Duigenan S, Oliva E, Lee SI. Ovarian torsion: Diagnostic features on CT and MRI with pathologic correlation. American Journal of Roentgenology 2012; 198(2): W122–W131.
22. Chang HC, Bhatt S, Dogra VS. Pearls and pitfalls in diagnosis of ovarian torsion. Radiographics 2008; 28(5): 1355–1368.
23. Pena JE, Ufberg D, Cooney N, *et al.* Usefulness of Doppler sonography in the diagnosis of ovarian torsion. Fertility and Sterility 2000; 73(5): 1047–1050
24. Chiou SY, Lev-Toaff AS, Masuda E, *et al.* Adnexal torsion: new clinical and imaging observations by sonography, computed tomography, and magnetic resonance imaging. Journal of Ultrasound in Medicine 2007; 26(10): 1289–1301.
25. Wilkinson C, Sanderson A. Adnexal torsion—A multimodality imaging review. Clinical Radiology 2012; 67(5): 476–483.
26. Lee EJ, Kwon HC, Joo HJ, *et al.* Diagnosis of ovarian torsion with color Doppler sonography: Depiction of twisted vascular pedicle. Journal of Ultrasound in Medicine 1998; 17(2): 83–89.
27. Albayram F, Hamper UM. Ovarian and adnexal torsion: Spectrum of sonographic findings with pathologic correlation. Journal of Ultrasound in Medicine 2001; 20(10): 1083–1089.
28. Lourenco AP, Swenson D, Tubbs RJ, *et al.* Ovarian and tubal torsion: Imaging findings on US, CT, and MRI. Emergency Radiology 2014; 21(2): 179–187.
29. Rha SE, Byun JY, Jung SE, *et al.* CT and MR imaging features of adnexal torsion. Radiographics 2002; 22(2): 283–294.
30. Hiller N, Appelbaum L, Simanovsky N, *et al.* CT features of adnexal torsion. American Journal of Roentgenology 2007; 189(1): 124–129.
31. Rajkotia K, Veeramani M, Macura KJ. Magnetic resonance imaging of adnexal masses. Topics in Magnetic Resonance Imaging 2006; 17(6): 379–397.
32. Moribata Y, Kido A, Yamaoka T, *et al.* MR imaging findings of ovarian torsion correlate with pathological hemorrhagic infarction. Journal of Obstetrics and Gynaecology Research 2015; 41(9): 1433–1439.
33. Emans SJ, Laufer MR. Pediatric and adolescent gynecology. Baltimore, Md: Lippincott Williams & Wilkins; 2005. p. 369.
34. Hiller N, Sella T, Lev-Sagi A, *et al.* Computed tomographic features of tuboovarian abscess. The Journal of Reproductive Medicine 2005; 50(3): 203–208.
35. Jeong WK, Kim Y, Song SY. Tubo-ovarian abscess: CT and pathological correlation. Clinical Imaging 2007; 31(6): 414–418.
36. Lee DC, Swaminathan AK. Sensitivity of ultrasound for the diagnosis of tubo-ovarian abscess: A case report and literature review. Journal of Emergency Medicine 2011; 40(2): 170–175.
37. Wilbur AC, Aizenstein RI, Napp TE. CT findings in tuboovarian abscess. American Journal of Roentgenology 1992; 158(3): 575–579.
38. Ellis JH, Francis IR, Rhodes M, *et al.* CT findings in tuboovarian abscess. Journal of Computer Assisted Tomography 1991; 15(4): 589–592.
39. Eshed I, Halshtok O, Erlich Z, *et al.* Differentiation between right tubo-ovarian abscess and appendicitis using CT—A diagnostic challenge. Clinical Radiology 2011; 66(11): 1030–1035.
40. Noone TC, Semelka RC, Worawattanakul S, *et al.* Intraperitoneal abscesses: Diagnostic accuracy of and appearances at MR imaging. Radiology 1998; 208(2): 525–528.
41. Dohke M, Watanabe Y, Okumura A, *et al.* Comprehensive MR imaging of acute gynecologic diseases. Radiographics 2000; 20(6): 1551–1566.
42. Kim SH, Kim SH, Yang DM, *et al.* Unusual causes of tubo-ovarian abscess: CT and MR imaging findings. Radiographics 2004; 24(6): 1575–1589.
43. Bakir B, Bakan S, Tunaci M, *et al.* Diffusion-weighted imaging of solid or predominantly solid gynaecological adnexal masses: Is it useful in the differential diagnosis? British Journal of Radiology 2011; 84(1003): 600–611.
44. Fujii S, Kakite S, Nishihara K, *et al.* Diagnostic accuracy of diffusion-weighted imaging in differentiating benign from malignant ovarian lesions. Journal of Magnetic Resonance Imaging 2008; 28(5): 1149–1156.
45. Rezvani M, Shaaban AM, Kennedy AM. The role of multimodality imaging after cesarean delivery. Ultrasound Quaterly 2015; 31(1):5–18.
46. Brown CE, Stettler RW, Twickler D, *et al.* Puerperal septic pelvic thrombophlebitis: Incidence and response to heparin therapy. American Journal of Obstetrics and Gynecology 1999; 181(1): 143–148.
47. Josey WE, Staggers Jr SR. Heparin therapy in septic pelvic thrombophlebitis: A study of 46 cases. American Journal of Obstetrics and Gynecology 1974; 120(2): 228–233.
48. Garcia J, Aboujaoude R, Apuzzio J, *et al.* Septic pelvic thrombophlebitis: Diagnosis and management. Infectious Diseases in Obstetrics and Gynecology 2006; 2006: 1–4.
49. Kominiarek MA, Hibbard JU. Postpartum ovarian vein thrombosis: An update. Obstetrical & Gynecological Survey 2006; 61(5): 337–342.

50. De Cuyper K, Eyselbergs M, Bernard P, *et al.* Added value of diffusion-weighted MR imaging in the diagnosis of postpartum ovarian vein thrombosis. Jbr-btr 2014; 97(4): 242–244.
51. Kataoka ML, Togashi K, Kobayashi H, *et al.* Evaluation of ectopic pregnancy by magnetic resonance imaging. Human Reproduction 1999; 14(10): 2644–2650.
52. Della-Giustina D, Denny M. Ectopic pregnancy. Emergency Medicine Clinics in North America 2003; 21: 565–584.
53. Tamai K, Koyama T, Togashi K. MR features of ectopic pregnancy. European Radiology 2007; 17(12): 3236–3246.
54. Refaat B, Dalton E, Ledger WL. Ectopic pregnancy secondary to in vitro fertilization-embryo transfer: Pathogenic mechanisms and management strategies. Reproductive Biology and Endocrinology 2015; 13(1): 30.
55. Baron KT, Babagbemi KT, Arleo EK, *et al.* Emergent complications of assisted reproduction: Expecting the unexpected. Radiographics 2013(1); 33: 229–244.
56. Braffman BH, Coleman BG, Ramchandani P, *et al.* Emergency department screening for ectopic pregnancy: A prospective US study. Radiology 1994(3); 190: 797–802.
57. Condous G, Okaro E, Khalid A, *et al.* The accuracy of transvaginal ultrasonography for the diagnosis of ectopic pregnancy prior to surgery. Human Reproduction 2005; 20(5): 1404–1409.
58. Shalev E, Yarom I, Bustan M, *et al.* Transvaginal sonography as the ultimate diagnostic tool for the management of ectopic pregnancy: Experience with 840 cases. Fertility and Sterility 1998; 69(1): 62–65.
59. Brown DL, Doubilet PM. Transvaginal sonography for diagnosing ectopic pregnancy: Positivity criteria and performance characteristics. Journal of Ultrasound in Medicine 1994; 13(4): 259–266.
60. Sadek AL, Schiotz HA. Transvaginal sonography in the management of ectopic pregnancy. Acta Obstetricia et Gynecologica Scandinavica 1995; 74(4): 293–296.
61. Yoshigi J, Yashiro N, Kinoshita T, *et al.* Diagnosis of ectopic pregnancy with MRI: Efficacy of T2*-weighted imaging. Magnetic Resonance in Medical Sciences 2006; 5(1): 25–32.
62. Murase E, Siegelman ES, Outwater EK, *et al.* Uterine leiomyomas: Histopathologic features, MR imaging findings, differential diagnosis, and treatment. Radiographics 1999; 19(5): 1179–1197.
63. McLucas B. Diagnosis, imaging and anatomical classification of uterine fibroids. Best Practice & Research Clinical Obstetrics & Gynaecology 2008; 22(4): 627–642.
64. Furey EA, Bailey AA, Pedrosa I. Magnetic resonance imaging of acute abdominal and pelvic pain in pregnancy. Topics in Magnetic Resonance Imaging 2014; 23(4): 225–242.
65. Ueda H, Togashi K, Konishi I, *et al.* Unusual appearances of uterine leiomyomas: MR imaging findings and their histopathologic backgrounds. Radiographics 1999; 19(suppl.1): 131–145.
66. Potter AW, Chandrasekhar CA. US and CT evaluation of acute pelvic pain of gynecologic origin in nonpregnant premenopausal patients. Radiographics 2008; 28(6): 1645–1659.
67. Roy C, Bierry G, El Ghali S, *et al.* Acute torsion of uterine leiomyoma: CT features. Abdominal Imaging 2005; 30(1): 120–123.
68. Hueppchen N, Ling FW. Ectopic pregnancy and abortion. 6th ed. In: Beckmann CR, Ling FW, Smith RP, *et al.* (editors). Obstetrics and gynecology. Baltimore, Md: Lippincott Williams & Wilkins; 2010. p. 142–143.
69. Katz DS, Khalid M, Coronel EE, *et al.* Computed tomography imaging of the acute pelvis in females. Canadian Association of Radiologists Journal 2013; 64(2): 108–118.
70. Kim JC, Kim SS, Park JY. "Bridging vascular sign" in the MR diagnosis of exophytic uterine leiomyoma. Journal of Computer Assisted Tomography 2000; 24(1): 57–60.
71. Nishino M, Hayakawa K, Iwasaku K, *et al.* Magnetic resonance imaging findings in gynecologic emergencies. Journal of Computer Assisted Tomography 2003; 27(4): 564–570.
72. Grand DJ, Mayo-Smith WW, Woodfield CA. Practical body MRI: Protocols, applications and image interpretation. Cambridge: Cambridge University Press; 2012.
73. Walsh CA, Reardon W, Foley ME. Unexplained prelabor uterine rupture in a term primigravida. Obstetrics & Gynecology 2007; 109(2 Part 1): 455.
74. Pepin M, Schwarze U, Superti-Furga A, *et al.* Clinical and genetic features of Ehlers-Danlos syndrome type IV, the vascular type. New England Journal of Medicine 2000; 342(10): 673–680.
75. Khabbaz AY, Usta IM, El-Hajj MI, *et al.* Rupture of an unscarred uterus with misoprostol induction: Case report and review of the literature. Journal of Maternal-Fetal Medicine 2001; 10(2): 141–145.
76. Moshiri M, Osman S, Bhargava P, *et al.* Imaging evaluation of maternal complications associated with repeat cesarean deliveries. Radiologic Clinics of North America 2014; 52(5): 1117–1135.
77. Rodgers SK, Kirby CL, Smith RJ, *et al.* Imaging after cesarean delivery: Acute and chronic complications. Radiographics 2012; 32(6): 1693–1712.